Joint European Research Infrastructure network for Coastal Observatories

D9.1 : WP9 first scientific report - Description of data assimilation systems

Grant Agreement n° 262584
Project Acronym: JERICO

Project Title: Towards a Joint European Research Infrastructure network for Coastal Observatories

Coordination: P. Farcy, IFREMER,

jerico@ifremer.fr, www.jerico-fp7.eu:

Authors: G. Charria, S. Dobricic, W. Fu, M. Gunduz, G. Korres, S. Ponsar, J. Schulz-Stellenfleth, J. Sumihar, M. Verlaan,
Involved Institutions: IFREMER, CMCC, DMI, HCMR, MUMM, HGZ, DELTARES

Version and Date: 1.0, 04 May 2012

Table of Contents

TABLE OF CONTENTS 3

1. DOCUMENT DESCRIPTION 5

2. EXECUTIVE SUMMARY 7

3. INTRODUCTION 9

4. MAIN REPORT 10

4.1. Adriatic Sea (CMCC) 10

4.2. North Sea (DELTARES) 14

4.3. 4.1. North Sea (MUMM) 18

4.4. Aegean Sea (HCMR) 20

4.5. Baltic Sea (DMI) 24

4.6. Bay of Biscay (IFREMER) 27

4.7. North Sea (HZG) 30

5. CONCLUSIONS 33

REFERENCES 34

1. Document description

REFERENCES

Annex 1 to the Contract: Description of Work (DoW) version XX

Document information	
Document Name	D9.1 : WP9 first scientific report
Document ID	
Revision	
Revision Date	04 May 2012
Author	G. Charria, S. Dobricic, W. Fu, M. Gunduz, G. Korres, S. Ponsar, J. Schulz-Stellenfleth, J. Sumihar, M. Verlaan,
Security	

History			
Revision	**Date**	**Modification**	**Author**

Diffusion list				
Consortium beneficiaries	X			
Third parties				
Associated Partners				

2. Executive Summary

In WP9 the evaluation of existing and future coastal observational platforms will be performed by applying Observational System Experiments (OSEs) and Observational System Simulation Experiments (OSSEs) that use data assimilation systems based on high resolution coastal ocean models. Data assimilation systems cover a wide range of European coastal areas from the Mediterranean Sea to the Northern European Seas. In particular they are located in the Aegean Sea, the Adriatic Sea, the Bay of Biscay, the North Sea and the Baltic. In addition to different geographical coverage, data assimilation systems have a number of technical differences. Each system applies models that have different horizontal and vertical resolutions, formulations of the vertical coordinate system, physical parameterizations and even differ by the number and the type of the processes that are simulated. Furthermore, some data assimilation schemes use the Kalman Filter, while some others are based on the variational approach. Also assimilated coastal observational platforms differ significantly in different systems.

In the report we provide an overview of each data assimilation system. The report, therefore, describes the entire JERICO methodology for the estimation of the impact of coastal observational platforms and provides the basis for the comnparison between individual components.

In the future presentation of the results of OSE and OSSE experiments we will have to underline the large variability of geographical areas and methodologies used for the estimation of the impact of observational systems. In addition we will have to cover as much as possible different environmental problems that our systems should address, from short term forecast in emergency situations to long term monitoring programmes.

3. Introduction

In WP9 the evaluation of existing and future coastal observational platforms will be performed by applying Observational System Experiments (OSEs) and Observational System Simulation Experiments (OSSEs) that use data assimilation systems based on high resolution coastal ocean models. Data assimilation systems cover a wide range of European coastal areas from the Mediterranean Sea to the Northern European Seas. In particular they are located in the Aegean Sea, the Adriatic Sea, the Bay of Biscay, the North Sea and the Baltic. In addition to different geographical coverage, data assimilation systems have a number of technical differences. Each system applies models that have different horizontal and vertical resolutions, formulations of the vertical coordinate system, physical parameterizations and even differ by the number and the type of the processes that are simulated. Furthermore, some data assimilation schemes use the Kalman Filter, while some others are based on the variational approach. Also assimilated coastal observational platforms differ significantly in different systems.

Sections of the report will present different data assimilation systems. In each section the first subsection will describe the geographical set-up, the second the model configuration, the third the data assimilation scheme, and the forth the observational data platforms. In the conclusions we will summarise the description of the systems and discuss some issues related to the future OSE and OSSE experiments.

4. Main Report

4.1. Adriatic Sea (CMCC)

4.1.1 Geographical set-up

The Adriatic Sea located in the northern part of the Central Mediterranean, between the Italian peninsula and the Balkans. It has a highly variable depth varying from about 30 m in the Northern Adriatic to 1200 m in the Southern Adriatic (Figure 4.1.1). It is connected to the Mediterranean Sea through Otranto Strait. The Adriatic Sea is characterized by a large seasonal and spatial variability of the atmospheric forcing and the river discharge. In particular the large river discharge exceeds the evaporation and determines the estuarine like exchange with the Mediterranean Sea. The near surface circulation is mainly cyclonic with a permanent South Adriatic Cyclonic Gyre and the Middle Adriatic Cyclonic Gyre. The Mediterranean water inflow along the eastern coast, and the permanent Western Adriatic Current along the western coast is mainly determined by the salinity gradient due to the large river runoff at the northern coasts. The dense water generated during the winter in the Adriatic Sea outflows through the lower layer of the Otranto Strait and represents a significant source of dense water in the Eastern Mediterranean.

4.1.2 Model description

NEMO (Nucleus for European Modelling of the Ocean) is a free-surface, finite difference, primitive equation model (Madec, 2008). The model set-up in the Adriatic Sea has a constant grid resolution of 1/48^{o} along the longitudinal and latitudinal directions that corresponds to 1.8 and 2.3 km respectively. The model grid has 432 points in the zonal, and 331 in the meridional direction. In the vertical direction, it is configured with 120 unevenly spaced horizontal z-levels. The bottom topography is represented by the partial cell method. Vertical grid spacing is 1 m in the top 60 m, then increases to 9 m at 100 m depth and further to 50 m at the deepest point in the Adriatic Sea. The largest spacing of 70 m is in the Ionian Sea at the deepest point (2800 m). The very high vertical resolution and a large number of layers is a unique feature of this model. There are several reasons for this choice. For example, the high resolution in the top layers may resolve well the bottom flow in the Northern Adriatic. It also facilitates the simulation of the vertical mixing during the high stratification in summer. The use of z-coordinate system with the high resolution may further improve the simulation of the spreading of water masses without excessive mixing. It should be mentioned that often sigma vertical coordinate is assumed to be more suitable for simulation of processes in shallow waters (e.g. Mellor et al., 2002). However, the combination of high vertical resolution and the partial cell implementation could significantly improve the performance of a z-coordinate model (e.g. Adcroft et al., 1997).

Initial conditions for temperature and salinity were derived from SeaDatanet climatology [ref]. The horizontal resolution of the climatology is 0.25^{o}. Although, the climatology has a coarse horizontal and vertical resolution, it was found that a few months after the start of the model integration fine scale structures developed (not shown). Model bathymetry is based on 75' regional bathymetry (M. Rixen, NURC, http://mseas.mit.edu/download/phaley/Adriatic/. This bathymetry was available only north from 40^{o}N. It was extended to the south by combining it with the Mediterranean Forecasting System (MFS) 1/16^{o} operational model bathymetry developed for the MFS basin scale model.

The horizontal eddy diffusivity for tracers and the horizontal viscosity coefficient for the dynamics use bilaplacian operator. The vertical mixing is parametrized by the Turbulent Kinetic Energy (TKE) scheme embedded in the NEMO model. The model applies the implicit scheme for the adjustment of the sea level. Although it dumps significantly fast barotropic oscillations, we assume that it is adequate for the simulation of the interaction between the baroclinic and barotropic processes.

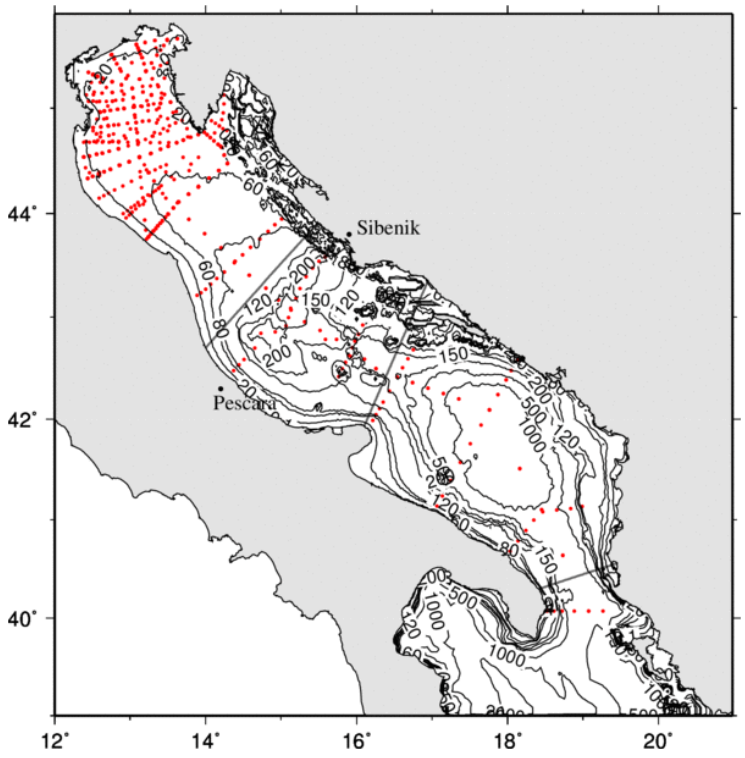

Figure 4.1.1: Horizontal domain and the bottom topography of the Adriatic model. Red dots represent historical CTD observations assimilated during the period 2000-2007. Horizontal lines divide the Adriatic into the north, middle and southern parts.

The river discharge has a large seasonal and monthly variability. Therefore, a proper representation of the rivers is important for simulating physical processes in the Adriatic Sea. The model uses monthly climatological values of river discharge for all rivers except for the Po river, for which daily values have been used. The Po river discharge is further divided into four branches. The river discharge values in the Adriatic Sea were obtained by combining the monthly climatological database by Raicich (1994), and by (Pasaric 2004). Special treatment of the river discharge has been implemented by increasing the diffusion at the upper 10 meters at the river mouth. In total there are 62 rivers.

Atmospheric forcing fields, except for precipitation, were obtained from the European Centre for Medium-Range Weather Forecasts (ECMWF) ERA-Interim data set. The precipitation was obtained from the Merged Analysis of Precipitation (CMAP) observational data set (Xie and Arkin 1997). The ERA-Interim atmospheric forcing fields are available at the frequency of 6 hour and the horizontal resolution of 0.25 °. The monthly mean CMAP data set has the horizontal resolution of 2.5 °.

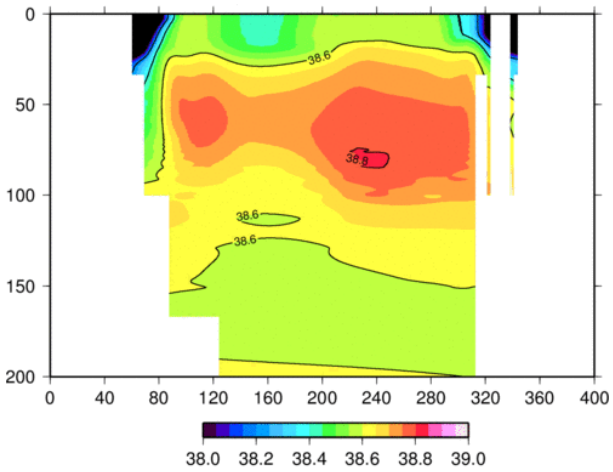

Figure 4.1.2: Simulated salinity along the transect between Pescara and Sibenik in September 2003. Due to the very high vertical resolution of the model and the use of the z vertical coordinate it was possible to simulate the advection of the highly saline Mediterranean waters into the Northern Adriatic. This process is frequently observed in the Adriatic, but it was difficult to simulate by the previous simulations.

The model set-up has one open boundary communicating with the Mediterranean Sea positioned south of the Otranto Strait.(see Figure 4.1.1). The boundary conditions for temperature, salinity, sea surface height, zonal and meridional currents are provided daily from outer basin scale MFS Mediterranean Model. The model uses scale selective open boundary conditions.

4.1.3 Data assimilation scheme

The MFS data assimilation system consists of the Adriatic set-up of the NEMO ocean model (Gunduz et al. 2012) and the OceanVar data assimilation scheme (Dobricic and Pinardi 2008). In the OceanVar set-up the slowly evolving vertical part of temperature and salinity background error covariances is represented by monthly varying Empirical Orthogonal Functions (EOFs). They are calculated in each model point separately by the method described in Dobricic et al. (2006).

The horizontal part of background error covariances is assumed to be Gaussian isotropic depending only on distance. It is modeled by the successive application of the recursive filter in longitudinal and latitudinal directions, that provides a high computational efficiency in each iteration of the algorithm. The rapidly evolving part of the background error covariances, consisting of the sea level and the barotropic velocity components, is modeled in each step of the minimization algorithm by applying a barotropic model forced by the vertically integrated buoyancy force resulting from temperature and salinity variations. The velocity is then estimated by applying the geostrophic relationship, modified along the coast by the application of the divergence dumping filter in order to eliminate the horizontal divergence. In this way OceanVar combines long term three dimensional variational scheme for the slow processes with a scheme that fully dynamically evolves the covariances by model equations for the fast processes. In particular the dynamical model used for the simulation of covariances between sea level errors and errors in temperature and salinity fields allows their very accurate estimate over areas with highly variable or shallow bottom topography typical for coastal areas.

4.1.4 Observational data sets

Currently the Adriatic system assimilates in situ observations of temperature and salinity by Argo floats, XBT instruments, CTD profiles by near-coastal observatories, observations of positions of Argo floats and surface drifters. It also assimilates satellite observations of Sea Surface Temperature (SST and Sea Level Anomaly (SLA). All in situ and satellite observations currently assimilated are available at the CMCC. During Jerico the observations by voluntary fishing boats will be assimilated in OSE experiments. They will be provided by the CNR. The observations of drifting floats for the OSSE experiments will be provided by the OGS.

Satellite observations of the SST are available from the CNR, and observations of SLA by the CLS. The background SLA estimate is formed by subtracting the Mean Dynamic Topography (MDT) estimate from the background sea level estimate. The MDT is obtained by combining the estimate by Rio et al. (2007) for the Southern Adriatic Sea with the information from the in situ observations in a procedure similar the one applied in Dobricic (2005). The Rio MDT estimate is not available for the Northern Adriatic, and therefore the SLA is assimilated only in the Southern Adriatic up to 42^{o}N. In the assimilation scheme the mean residual is subtracted from the residuals along each SLA satellite track. In this way the unknown steric height signal is removed together with the largest scale oscillations that may originate from the atmospheric pressure forcing or from other atmospheric processes. Residuals are calculated at the observational time.

4.2. North Sea (DELTARES)

4.2.1 Geographical set-up

The North Sea is located between Great Britain, Belgium, the Netherlands, Germany, and Scandinavia. It connects to the Atlantic Ocean through the English Channel in the south and the Norwegian Sea in the north. In the east, it connects to the Baltic Sea. The main pattern of water flow in the North Sea is anti clockwise rotation along the edges. It receives the majority of ocean current from the northwest opening and a smaller portion from the opening at the English Channel.

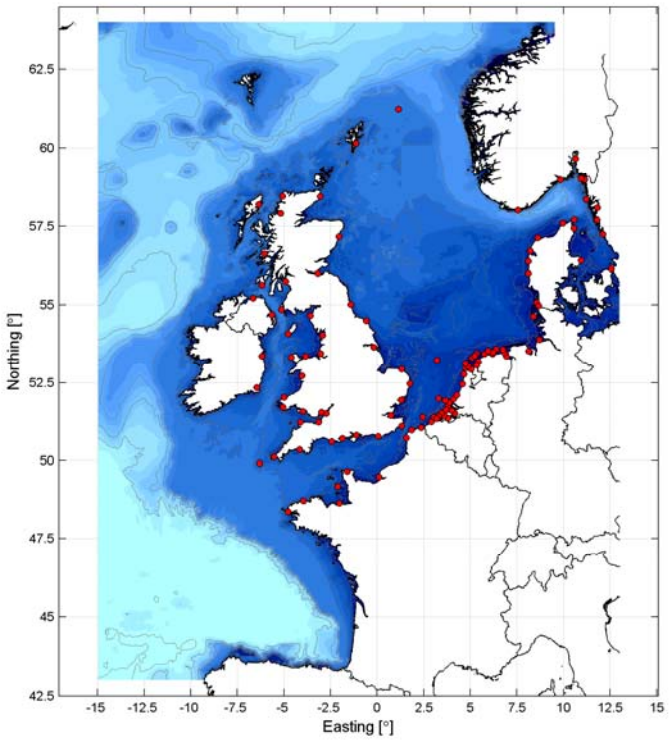

Figure 4.2.1: DCSMv6 area and overview of tide gauge stations available for calibration and validation

4.2.2 Model description

Currently, a sequence of models (DSMv5, ZUNOv4, Kuststrook Fijnv6) is used operationally for water level forecasts in the North Sea (Verlaan et al. 2005). These models will be replaced by the new generation DCSMv6 model (Zijl et al. 2008).

DCSMv6 has been developed as an application of SIMONA, a framework for hydrodynamic modelling of free-surface water systems. Within the SIMONA framework, the WAQUA module is used for modelling 2D (horizontal) schematizations of water systems. DCSMv6 uses spherical grid that has a uniform cell size of 1.5' (1/40°) in east-west direction and 1.0' (1/60°) in north-south direction. This corresponds to a grid cell size of about 2 by 2 km. The grid is specified in geographical coordinates and covers the area between 15° W to 13° E and 43° N to 64° N (Figure 4.2.1). The model area of DCSMv6 has been extended in order to ensure that the open boundary conditions are located further away in deep water. This makes it possible to use harmonic boundary forcing derived from global tidal models. Furthermore, wind setup in deep water can safely be neglected, whereas the effect of local pressure (the so-called inverse barometer effect) is added to the water level variation along the open boundary.

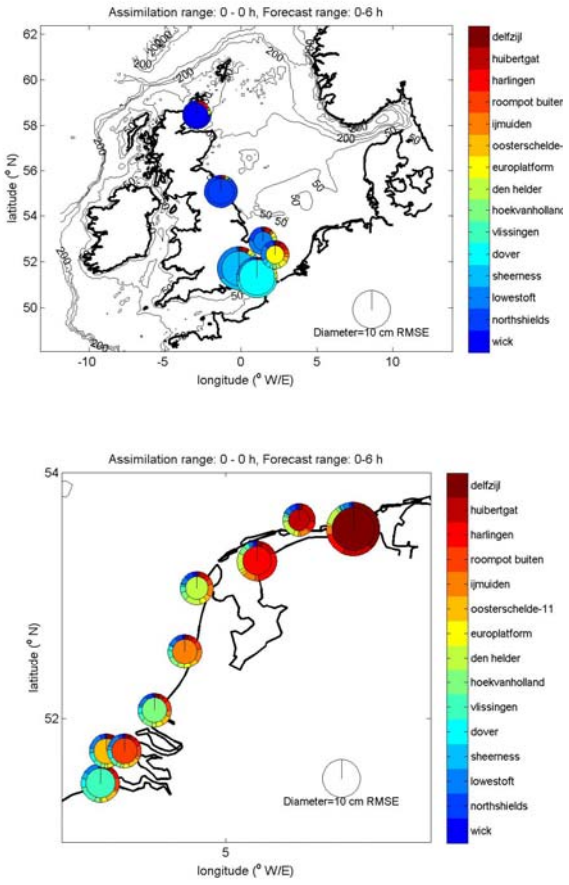

Figure 4.2.2: Observation impact estimate, averaged over the first six hours forecast horizon, along the British coast (top) and the Dutch coast (bottom). At each location, the area of larger circle represents the cost of without data assimilation, the inner smaller circle with data assimilation, and each colored segment in between the two circles represents the contribution to the cost reduction of the respective assimilation station listed on the color bar. The diameter of each circle represents the RMS of water level residual.

The model bathymetry is specified on the cell corners of the DCSMv6 model grid. Depths at the location of the cell centres (where water levels are specified and computed) are determined by using the mean value of the surrounding values at the cell corners. The DCSMv6 area covers an area where bathymetry varies from more than 2000 meter in the northern part down to less than 50 meter in the southern North Sea.

At the northern, western and southern sides of the model domain, open water level boundaries are defined. Water levels are specified at 205 different locations along those boundaries. In between these locations the imposed water levels are interpolated linearly. The imposed water levels at the open boundaries can be splitted in tidal and non-tidal components. The tidal water levels at the open boundaries are specified in terms of amplitudes and phases of a number of tidal constituents are specified. The tidal conditions of the eight main diurnal and semi-diurnal constituents have been derived by interpolation from a dataset derived from the GOT00.2 global tidal model. These eight tidal constituents (in order of increasing angular velocity) are Q1, O1, P1, K1, N2, M2, S2 and K2. Some smaller diurnal and semi-diurnal constituents have been added later. These smaller constituents have been derived from the eight main constituents by means of the admittance method. The smaller constituents added are MU2, NU2, LABDA2, T2, 2Q1, SIGMA1, RO1, M1, CHI, PI1, FI1, THETA1, J1, OO1, 2N2 and L2. In addition, the annual constituent Sa is also used; this has been determined from satellite altimetry data. While wind setup at the open boundary is neglected because of the deep water there, the (non-tidal) effect of local pressure can be significant. This so-called inverse barometer effect varies in time and space (dependent on the local atmospheric pressure) and is added to the tidal water level variation along the open boundary.

Tide Generating Forces (TGF), recently implemented in SIMONA, have been switched on in the DCSMv6 model. The effect of TGF has an amplitude in the order of 10 cm throughout the model domain (determined with a preliminary version of the model). Components of the tide with a Doodson number from 55.565 to 375.575 have been included. Consequently, the constituents M0 and S0, which would have caused a static elevation that varies in space, are excluded.

For meteorological forcing of the DCSMv6 model use has been made of time- and space varying wind (at 10 m height) and pressure (at MSL), derived from HIRLAM. For the calibration and validation of DCSMv6 hindcast data from HIRLAM version v7.0 is used, with output available every 3 hours. For interpolating the wind and pressure fields on the DCSMv6 grid, the HIRLAM land-sea mask has been taken into account. Cells that are more than 50 % land are excluded from the HIRLAM wind and pressure fields and where necessary extrapolated based on the data at surrounding points.

4.2.3 Data assimilation scheme

Like in the current operational system, a data assimilation procedure based on a steady state Kalman filter will be implemented with the DCSMv6 model. The steady state Kalman filter will assimilate 10-minutely in situ observed water level data into the DCSMv6, with a hindcast-forecast cycle of six hours.

In the Kalman filter, it is assumed that the source of uncertainty is due to the wind input. An autoregressive model AR(1) is used to represent this error process. Further, the covariance of this error is assumed to be isotropic in space and constant in time. As for the observational error, a Gaussian white noise with standard deviation of five centimeter is assumed for each observation.

The steady state Kalman gain will be determined by using an ensemble Kalman filter. First, an ensemble Kalman filter with the above-mentioned error specifications will be used with the DCSMv6 off-line, to generate a series of Kalman gains at various time levels. The steady state Kalman gain will then be obtained by simply averaging these Kalman gains over time. The generic data assimilation software OpenDA (Verlaan, et al., 2010) is used both for the preparation of the Kalman gain as well as for the operational steady state Kalman filter.

4.2.4 Observational data sets

A large number of tide gauge measurements are available for the calibration and validation of DCSMv6 (Figure 4.2.1). An analysis method has been developed recently for estimating observation impact in a Kalman filter setup (Sumihar and Verlaan, 2010). This method will be used to select which of these stations are to be included for data assimilation.

The method estimates the impact of data assimilation on forecast accuracy, where the measure of forecast accuracy is defined as a quadratic cost function of observation-minus-model residuals. It uses simply timeseries of observation and the corresponding model output generated without data assimilation. Therefore, it is applicable even before a Kalman filter is actually implemented. For illustration, a result of such analysis for the present operational model DCSMv5 is shown in Figure 4.2.2.

4.3.4.1. North Sea (MUMM)

4.3.1 Geographical set-up

The North Sea domain under consideration is located between 4°W to 10°E in longitude and 48.5°N to 60°N in latitude. There are three open sea boundaries: a narrow connection to the English Channel through the Dover Strait, a connection to the Baltic Sea through the Skagerrak, and a wide northern boundary. Its bathymetry varies widely, with large areas that are less than 40 meters deep (Southern and German Bights as well as the Dogger Bank) while there are deeper regions east and west of the Dogger Bank where the depths exceed 90 meters. Along the Norwegian Trench, the depth is up to 700 meters. The most important forcing mechanisms are the tides and the wind. Semi-diurnal tides are predominant at the latitude under consideration. The dominant factor governing the temperature field is the surface seasonal heating and cooling which, in the central part of the North Sea, leads to a thermal stratification of the water column in summer.

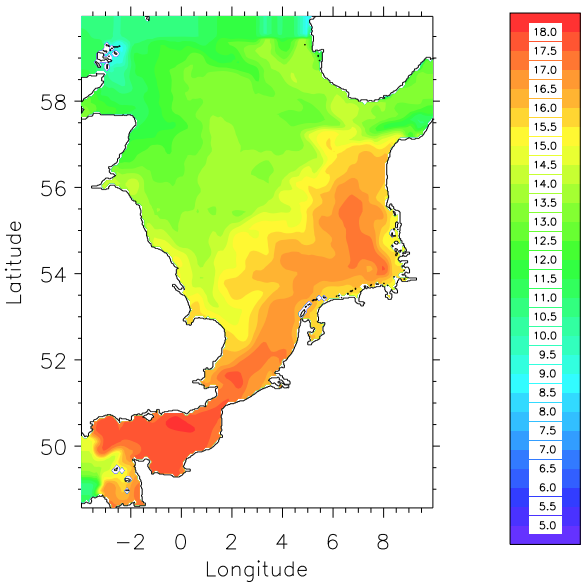

Figure 4.3.1: Surface temperature modelled without data assimilation on the last day of the assimilation period (September 28, 2001)

4.3.2 Model description

The COHERENS (Coupled Hydrodynamical-Ecological Model for Regional and Shelf Seas) model (Luyten, 2011) is a finite difference model. Simulations will be performed with a horizontal resolution of 4 nautical miles in the horizontal and 20 σ-sigma levels in the vertical for September 2001. Meteorological data are supplied by the Danish Meteorological Institute (DMI) from the HIRLAM model with a temporal resolution of one hour. Tidal harmonics and daily profiles of currents, temperature, salinity and inflow/outflow conditions at the boundaries of the domain are derived from simulations with the POLCOMS (Proudman Oceanographic Laboratory) model covering a larger area.

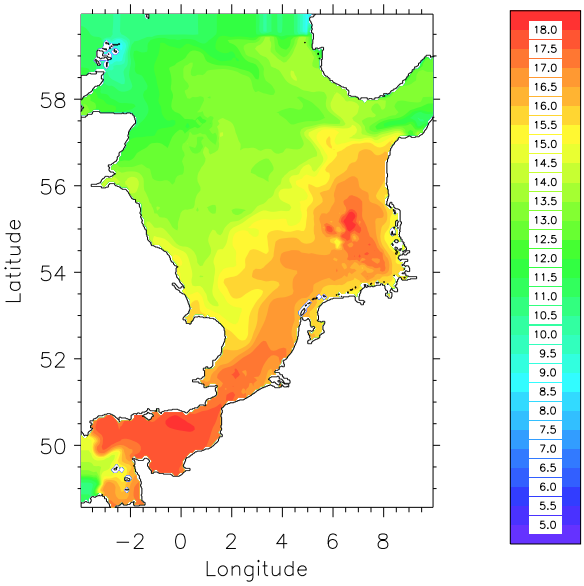

Figure 4.3.1: Surface temperature modelled with data assimilation on the last day of the assimilation period (September 28, 2001)

River runoffs from the Elbe, Scheldt, Rhine/Meuse, Thames, Humber, Tyne/Tees are taken into account. Baroclinic inflow/outflow conditions are imposed at the eastern boundary to include the exchange of water masses with the Baltic Sea.

4.3.3 Data assimilation scheme

The ensemble Kalman filter developed by Evensen, (1994) combines the traditional Kalman filter with Monte-Carlo methods to generate an ensemble of states representing the model error. A low rank square root algorithm allowing an ensemble representation of the observations' error is applied at the analysis step.

An initial ensemble of states is generated from the 1st of September and is integrated without data assimilation till the 11th of September. The model error is sampled once a day using 50 ensemble members. Eight temperature profiles are assimilated once a day at midnight from the 12th of September till the 28th of September. They are extracted at the assimilation time step from model runs generated with the same set-up but with a higher horizontal resolution of one nautical mile. Their impact on the neighboring temperature field is limited by means of an assimilation cutoff radius.

4.3.4 Data sets that will be assimilated

Four data sets of eight synthetic temperature profiles are assimilated. They represent four observational networks whose impact on the modelled temperature will be assessed and compared.

4.4. Aegean Sea (HCMR)

4.4.1 Geographical set-up

The Aegean Sea model domain covers the geographical area 19.5oE – 30oE and 30.4oN – 41oN (Figure 4.4.1) with a horizontal resolution of 1/30o and 25 sigma layers along the vertical with a logarithmic distribution near the surface and the bottom. The model includes parameterization of fresh water discharge from major Greek rivers (Axios, Aliakmonas, Nestos, Evros) while the inflow/outflow at the Dardanelles is treated with open boundary techniques (Korres et al., 2002).

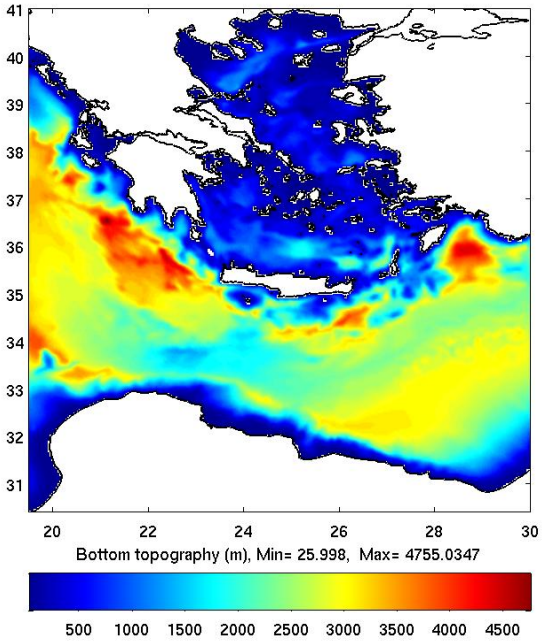

Figure 4.4.1: The Aegean Sea model domain and bathymetry

The Dardanelles outflow into the Aegean Sea is a dominant factor for the freshwater budget of the basin providing approximately 300 km3 of brackish water on an annual basis. The main Greek rivers (Axios, Aliakmonas, Gallikos, Pinios, Sperchios, Evros, Strimonas and Nestos) on the other hand with a total runoff of ~19 km3/yr have a much less contribution to the freshwater budget. Even lower is the contribution of the Turkish rivers with a total runoff of ~5 km3/yr. The Strait of Dardanelles is treated as an open boundary where a two layer system is explicitly prescribed with inflow of fresh Black Sea Water (BSW) in the upper layer and outflow of saline Aegean waters below. The inflow/outflow transports follow a seasonal cycle with maximum values of inflow to the Aegean during mid-March (0.037 Sv) and minimum during mid-July (0.027 Sv) while the net transport follows the pattern of Kanarska and Maderich (2008). The salinity of the upper layer is set to 28.3 psu with a seasonal variation of 2 psu while the interface depth is kept fixed to 25m.

Boundary conditions at the western and eastern open boundaries of the Aegean Sea hydrodynamic model are provided on a daily basis (daily averaged fields) by the Mediterranean Ocean Forecasting system. The nesting between the two models involves the zonal/meridional external (barotropic) and internal velocity components, the temperature/salinity profiles and the free surface elevation following the nesting procedures described in Korres and Lascaratos (2003). Additionally, volume conservation constraints between the two models are applied at both open boundaries of the Aegean Sea model.

4.4.2 Model description

The Aegean Sea model is based on the Princeton Ocean model (POM) and was developed as part of the Poseidon system (Soukissian et al., 2002). POM is a primitive equations ocean model which operates under the hydrostatic and Boussinesq approximations. The model equations are written in sigma-coordinates and discretized using the centered second-order finite differences approximation in a staggered "Arakawa C-grid" with a numerical scheme that conserves mass and energy. The spatial differences are central and explicit in the horizontal and implicit in the vertical. Centered differences (leapfrog scheme) are used for the time integration of the primitive equations. Additionally, since the leapfrog scheme has a tendency for the solution to split at odd and even time steps, an Asselin filter is used at every time step. The prognostic variables of the model are the sea surface elevation ζ, the zonal u and meridional v components of velocity (the vertical

velocity is solved diagnostically) and their depth-averaged counterparts ($\bar{u}$,$\bar{v}$), potential temperature T, salinity

S, the turbulent kinetic energy q^2 and the turbulent kinetic energy times the length scale q^2 l. The model is forced with hourly surface fluxes of momentum, heat and water provided by the Poseidon - ETA high resolution (1/10o) regional atmospheric model (Papadopoulos et al., 2002) issuing forecasts for 72 hours ahead.

4.4.3 Data assimilation scheme description

The assimilation scheme used by the Aegean Sea forecasting system, is based on the Singular Evolutive Extended Kalman (SEEK) filter which is an error subspace extended Kalman filter that operates with low-rank error covariance matrices as a way to reduce the prohibitive computational burden of the extended Kalman filter (Pham et al., 1997). The filter is additionally implemented with covariance localization and partial evolution of the correction directions. More specifically, a linear operator is defined that restricts the global observation vector to its local part according to some cut-off radius (radius of influence) which is set (upon sensitivity experiments) to 200 km. The approximation of "partial evolution" of the correction directions was first proposed by Hoteit et al. (2002, 2003) and subsequently by Korres et al. (2009) who found that this approach has a limited impact on the filter performance. Partial evolution of the correction directions significantly reduces the computational cost of the SEEK filter making it more suitable for operational systems. Moreover it is very similar with the hybrid Kalman filtering approach followed in various studies. Its use in the high resolution Aegean Sea model can be further supported by the fact that the evolution of the last (i.e. least

significant) EOFs in the SEEK filter can be problematic and might introduce noise in the filter correction directions, and this was observed in preliminary experiments. In the Aegean Sea data assimilation system, the error covariance matrix is approximated by 60 EOF modes, the first 10 of which are evolved by the model following the Aegean Sea hydrodynamics.

To implement the SEEK filter, one first needs to initialize the recursive algorithm with a state estimate and a low rank (60 in our case) error covariance matrix P_0. One common way is to apply an Empirical Orthogonal Functions (EOF) analysis on a historical set S of system states (often model outputs) to determine a low-rank approximation of the sample covariance matrix of S as L_0 U_0 L_0^T. These smaller size matrices and the mean of the historical run are then used to start the SEEK filter.

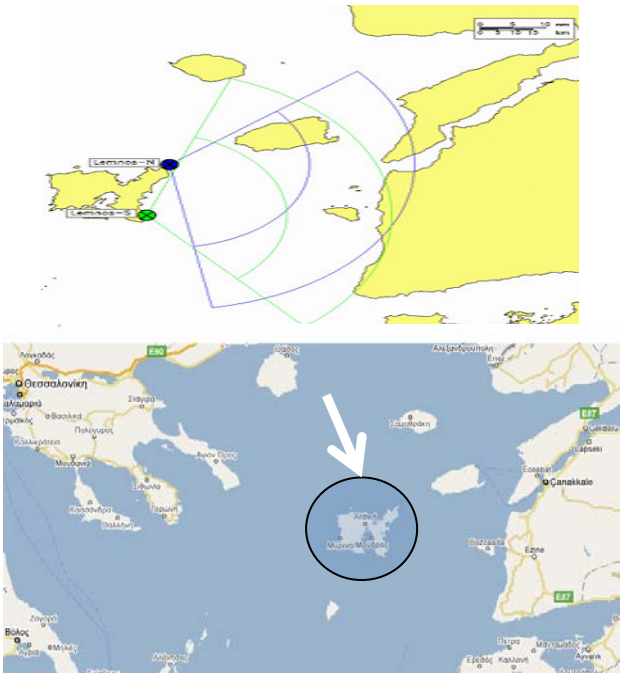

Figure 4.4.2: The HF radar system at the eastern coast of Lemnos island

In the framework of the CORI (Prevention and Management of Sea Originated Risks to the Coastal Zone) INTEREG IIIB ARCHIMED 2000-2006 programme, the University of the Aegean and the Hellenic Centre for Marine Research jointly installed a WERA HF radar system at the eastern coast of the island of Lemnos (Zervakis et al., 2011) facing the Dardanelles Straits (Figure 4.4.2). It uses a WERA HF Remote Sensing system (Helzel Messtechnik GmbH, Germany) transmitting electromagnetic waves in the range of 6 - 30 MHz to measure surface current velocities in the area. The shore-based antennas at the two sites (Plaka and Fisini) provide continuous temporal and broad spatial surface current observations, facilitating the delivery of data in near real-time and in high spatial and temporal resolution.

4.4.4 Data sets that will be assimilated

HF radars are capable of producing current vector maps of the coastal zone over spatial scales ranging from hundreds of meters to hundreds of kilometres and on time intervals from tens of minutes to days. The measurement is based on the fact that electromagnetic radiation in the 3- to 30-MHz range scatters strongly (Bragg scattering) from ocean surface gravity waves. The returned energy spectrum thus indicates movement of ocean surface gravity waves with a wavelength of half the radar-transmitted wavelength in directions either toward or away from the HF radar site. Subtraction of the theoretical phase velocity of the ocean waves gives radial current velocities (hereafter referred to as radials). Multiple radars are typically deployed so there is enough angular separation to resolve both the north–south and east–west velocity components. The initial planning required that the range of the system extends to the mouth of the Strait, in order to be able to separate the Dardanelles Current from a very energetic anticyclone that often contributes to the current through the Lemnos - Imvros channel. The HF system has been in operation since October 2009, and preliminary analysis of the data reveals that the system fulfills the above requirement about 30% of the time. Furthermore, the range of the system appears to vary depending on weather conditions.

4.5. Baltic Sea (DMI)

4.5.1 Model description

The physical model used in DMI's data assimilation is a two-way nested, free surface, hydrostatic three-dimensional (3D) circulation model HIROBM-BOOS (HBM). The model code forms the basis of a common Baltic Sea model for providing GMES Marine Core Service since 2009. The finite difference method is adopted for its spatial discretization in which a staggered Arakawa C grid is applied on a horizontally spherical and vertically z-coordinate. A detailed description of the model can be found in Berg and Poulsen (2011).

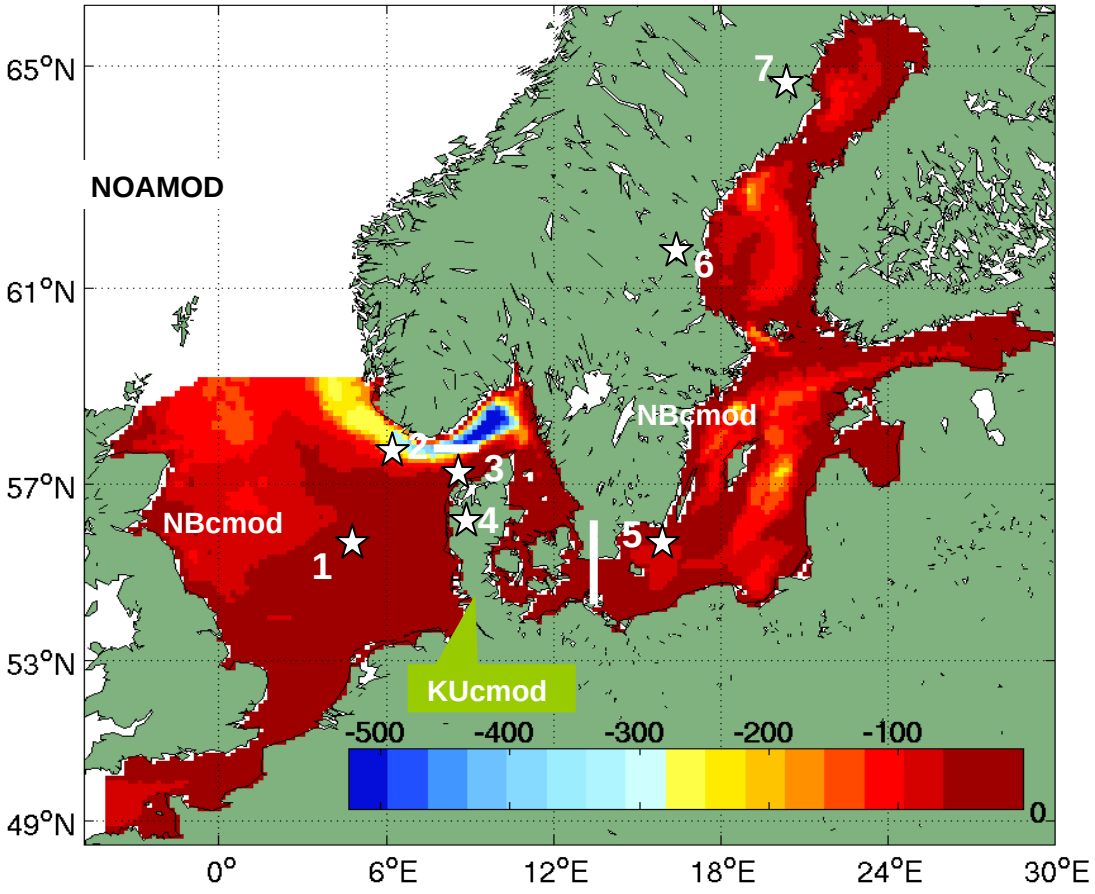

Figure 4.5.1: Two-way nested model domain together with bathymetry used in the physical model (HIROM) of DMI's data assimilation system. NOAMOD provides surge boundary conditions for the 3D North/Baltic Sea model, in the Danish water, a high resolution KUcmod is two-way

nested to the NBcmod.

The model is set up with a coarser resolution than the model's operational set up. It has a 6 nautical mile (nm) horizontal resolution for the Baltic-North Sea with a two-way nested 1nm resolution domain to resolve the narrow Danish Straits (Figure 4.5.1). It should be noted that the two-way nesting facility is very important in making multi-decadal simulations in order to correctly resolve the Baltic-North Sea transport. The 3D models have in total 50 vertical layers. The top layer thickness is selected at 8 m in the coarse resolution Baltic-North Sea model in order to avoid tidal drying of the first layer in the English Strait. The rest of the layers in the upper 80 m have 2 m vertical resolution. The layer thickness below 80 m increases gradually from 4 m to 50 m. For the fine resolution domain, the vertical resolution is enhanced to resolve the strong stratification in the shallow inner Danish waters. The top layer is 2 m and then with a 1 m or 2 m layer thickness in the rest of 49 layers.

The meteorological forcing is based on a reanalysis using the regional climate model HIRHAM through a dynamic downscaling (including a daily re-initialization) from ERA-Interim Global reanalysis. HIRHAM is a regional atmospheric climate model (RCM) based on a subset of the HIRLAM and ECHAM models, combining the dynamics of the former model with the physical parameterization schemes of the latter. The HIRLAM model – High Resolution Limited Area Model - is a numerical short-range weather forecasting system developed by the international HIRLAM Programme (http://hirlam.org). The ECHAM global climate model (GCM) is a general atmospheric circulation model developed at the Max Planck Institute of Meteorology (MPI) in collaboration with external partners. The original HIRHAM model was collaboration between DMI, the Royal Netherlands Meteorological Institute (KNMI) and MPI. A detailed description of HIRHAM Version 5 can be found in Christensen et al. (2006).

4.5.2 Data assimilation scheme

In this study, a 3DVAR is used to find the optimal solution of the model state **x** which minimizes the following cost function:

$$J(\mathbf{x}) = \frac{1}{2}(\mathbf{x}-\mathbf{x}_b)^T \mathbf{B}^{-1}(\mathbf{x}-\mathbf{x}_b) + \frac{1}{2}(H(\mathbf{x})-\mathbf{y}_o)^T \mathbf{R}^{-1}(H(\mathbf{x})-\mathbf{y}_o) \qquad (1)$$

x is the model state to be estimated. $\mathbf{x}_b$ is the background state vector, $\mathbf{y}_o$ is the observation state vector. H is the non-linear observational operator with which the analysis equivalent of observation $\mathbf{y} = H(\mathbf{x})$ can be obtained to compare with the observation measurements. The superscript T denotes matrix transpose. In the cost function, background error covariance (**B**) and observational error covariance (**R**) weight the misfit between analysis and background and the misfit between analysis and observation, respectively. Usually the optimal solution is found by minimizing the cost function $J(\mathbf{x})$ with respect to $\mathbf{x}$, in which its gradient is also needed for determining the search direction and iteration steps in the minimizing algorithm:

$$\nabla J(\mathbf{x}) = \mathbf{B}^{-1}(\mathbf{x} - \mathbf{x}_b) + \nabla_x H(\mathbf{x})^T \mathbf{R}^{-1}(H(\mathbf{x}) - \mathbf{y}_o) \quad (2)$$

An incremental method (Courtie et al, 1994) is used to transform Equation (1) and it is linearized around the background state into the following form:

$$J(\delta\mathbf{x}) = \frac{1}{2}\delta\mathbf{x}^T \mathbf{B}^{-1}\delta\mathbf{x} + \frac{1}{2}(\mathbf{H}\,\delta\mathbf{x} - \mathbf{d})^T \mathbf{R}^{-1}(\mathbf{H}\,\delta\mathbf{x} - \mathbf{d}) \quad (3)$$

where $\mathbf{d} = \mathbf{y}_o - \mathbf{H}(\mathbf{x_b})$ is the innovation vector, $\mathbf{H}$ is the linearized observation operator evaluated at $\mathbf{x} = \mathbf{x_b}$ and $\delta\mathbf{x} = \mathbf{x} - \mathbf{x_b}$ is the analysis incremental vector.

In our current scheme, the state vector is composed of only temperature and salinity model state variables:

$$\mathbf{x} = [T \quad S]^T \quad (4)$$

A preconditioned control variable transform (defined by $\delta\mathbf{x} = \mathbf{U}\mathbf{v}$) is used in the process of minimization (e.g. Lorenc, 1997) where $\mathbf{U}$ is chosen to approximately satisfy the relationship $\mathbf{B} = \mathbf{U}\mathbf{U}^T$ and the control variable vector $\mathbf{v}$ is chosen as their errors are relatively uncorrelated. In this way, the minimization can be carried out without handling the inverse of **B**. For a typical coastal ocean data assimilation system, the order of original size of the background error covariance matrix **B** is about 10^6~10^7. A quasi-Newton L-BFGS algorithm (Byrd et al. 1995) is adopted to minimize the cost function. Due to its moderate memory requirement, the L-BFGS method is particularly well suited for optimization problems with a large number of variables.

The computation of **B** implicitly involves the transform of **U** which includes a sequence of linear operators:

$$\mathbf{U} = \mathbf{U}_P \mathbf{U}_V \mathbf{U}_H \quad (5)$$

where $\mathbf{U}_H$ and $\mathbf{U}_V$ are the horizontal and vertical part of the control variable transform related to the modes of **B**, and $\mathbf{U}_P$ is the physical transform related to the multivariate dynamic or physical constraints (e.g. the relationship between sea surface height (SSH) error and temperature/salinity error).The horizontal part of background error covariance (B) is represented by recursive filter and the vertical part is represented with dominant EOF modes to reduce computational expense. A more detailed description is given in Zhuang et al (2011).

4.5.3 Observational data sets

At present, the system mainly assimilates satellite SST, historical T and S profiles from the International Council for the Exploration of the Sea (ICES), and sea ice concentration of the MyOcean products.

4.6. Bay of Biscay (IFREMER)

4.6.1 Geographical set-up

The Bay of Biscay, located in the Eastern part of the North Atlantic Ocean between the Spanish and the French coasts, is characterized by a narrow continental shelf in the South (30km) extending to a wide continental shelf (180km) off Brittany (Figure 4.6.1). This irregular and steep bathymetry combined with seasonal wind regimes and important river discharges in the frame of a large scale gyre circulation is driving a complex system of coastal currents (Charria et al., 2011). On the shelf, the currents may be explained as a combination of wind driven, tidally induced and density driven flows. The first order approximation shows that the circulation is mostly dominated by barotropic semidiurnal tides. More generally, on the continental shelf at lower frequency than the daily tidally driven circulation, residual currents are weak. On the Aquitaine shelf, the dynamics of the dominant winds (to the NE in winter and towards the SE the rest of the year) drives a weak complex seasonal circulation. In the vicinity of the estuaries (mainly Loire and Gironde), the freshwater discharges in the surface layers induce important density gradients driving a poleward circulation (about 10 cm s-1) modulated by the wind forcings. Further North, in the Iroise Sea, a combination of three physical processes is needed to explain current velocities in this region: semidiurnal tides, meteorological forcing, and strong thermal gradients in summer. Indeed, in this frontal region, a density-driven circulation is known to interfere with the currents induced by tide and atmospheric forcings. In some cases, the density-driven circulation can even preponderate over the barotropic tidal current.

4.6.2 Model description

MARS3D is a coastal model based on primitive equations (Lazure et Dumas, 2007). The model was designed to simulate flows in various coastal areas from the regional scale down to the inshore scale of small bays or estuaries where circulation is generally driven by a mix of processes. The processes to be modeled enable simplifications of the Navier–Stokes equations on the classic Boussinesq and hydrostatic hypotheses. These equations are transformed within a sigma framework to make free surface processing easier. A model specificity is the original aspect of the coupling between barotropic and baroclinic modes especially designed for ADI (semi-implicit method). It explains how full consistency of the transport calculated within the 2D and 3D equation sets was obtained.

The model set-up in the Bay of Biscay and the Channel has a constant grid resolution of 4Km. The model is using sigma vertical coordinates distributed along 30 levels.

The vertical mixing is parametrized by the Turbulent Kinetic Energy (TKE) scheme. The river discharge has a large seasonal and monthly variability. Therefore, a proper representation of the rivers is important for simulating physical processes in the Bay of Biscay. The model uses real-time measured river runoff for large rivers, watershed model for other rivers and a climatological annual cycle for missing real time river data.

Atmospheric forcing fields were obtained from the European Centre for Medium-Range Weather Forecasts (ECMWF) Analyses. Open boundaries conditions are provided by the MERCATOR-PSY2 North Atlantic model except for tides. Indeed, sea levels are calculated by a barotropic 2D model (MARS2D) deployed on larger domain than the Bay of Biscay configuration.

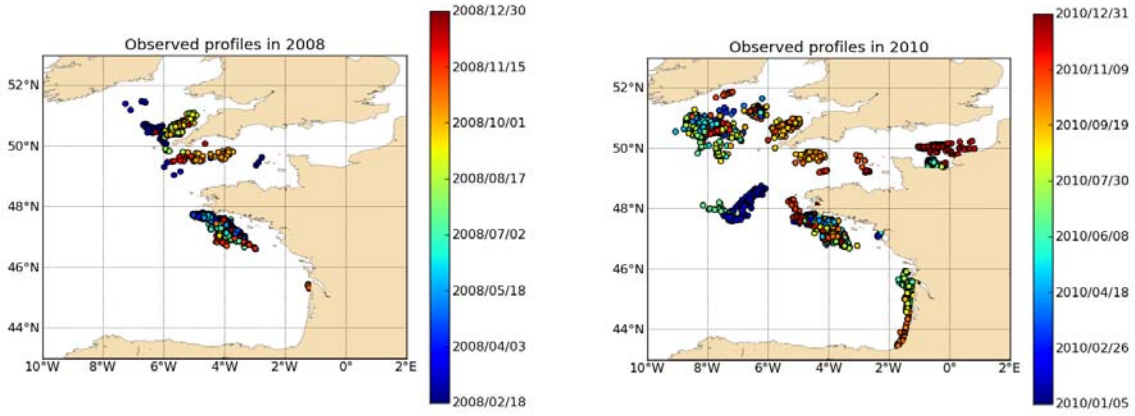

Figure 4.6.1: Collected qualified RECOPESCA profiles in 2008 (a) and 2010 (b).

4.6.3 Data assimilation scheme

For the present experiment, a method (Le Hénaff et al., 2009), based on ensemble approaches, has been retained. Based on the notion of array modes defined by Bennet (1985, 1990), the Representer Matrix Spectra (RMS) can be applied to optimize a network design without running a fully assimilated system.

The RMS method (Le Hénaff et al., 2009) allows estimating through an ensemble of simple qualitative and quantitative diagnostics the degrees of freedom of a model error subspace (Figure 4.6.2), which are observable and consequently controllable by a given observations network. Basically, this methodology is founded on a comparison of the model errors with the observation ones: if the model errors are greater than the observation errors, the information brought up by the network is theoretically useful to constrain or control the model; on the contrary, if the model error is weaker than the measurement error, the network does not bring any relevant information. This method is handful and easy to implement since it does not need, strictly speaking, any data assimilation phase, this latter process being generally time-consuming and complex to set up. The general methodology has already been described in details by Le Hénaff et al., 2009. Thus, we only remind here the main steps of the methodology.

The purpose of the method is to examine whether and under which circumstances one particular array (H;R) can be said to be "objectively satisfactory", and whether, given two arrays (H1;R1) and (H2;R2), one of them can be said to be more efficient than the other (H is the observation operator, which projects the state vector onto the observational space, and R is the covariance matrix of the observational errors).

Following Le Hénaff et al. (2009), this can be achieved through the comparison of the matrix HPgHT , known as the representer matrix (is the guess error covariance matrix) and the matrix R. If R dominates, the

discrepancies between the observations and the model are mostly due to observational errors, and the array is pretty much useless. If HPgHT dominates, then the discrepancies are mostly due to guess, and the observational array would probably be useful to assess and then possibly correct the model in a data assimilation step.

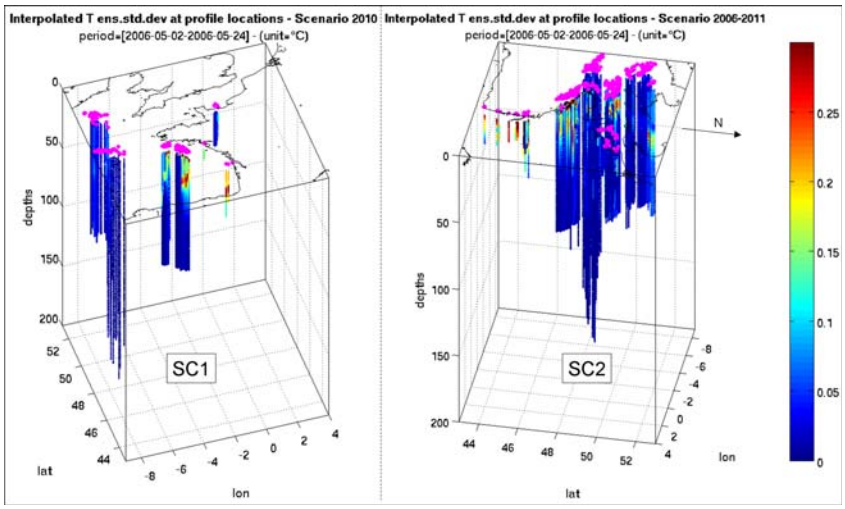

Figure 4.6.2: Model space-time interpolated error on profile locations of a network based on 2010 measurements (left) and the network based on 2006-2011 measurements (right) - position at surface (pink triangles) and at depth (colored dots) from 2nd to 24th May.

4.6.4 Observational data sets

Data used for this experiment are delivered by the RECOPESCA project. It provides an observation network, based on voluntary vessels, of the fisheries activity (effort and catches) and of environmental data. These measurements contribute to the evaluation of exploited resources and to the collection of new environmental data, as water temperature and salinity. Since 2004, the system is deployed on an increasing number of voluntary vessels. Specific sensors are implemented on the fishing gears and aboard a sample of vessels representative of the whole fishing fleets. These sensors have been developed to be suitable with conditions and constraints aboard fishing vessels (tough enough to be fixed up on fishing gears, self powered, autonomous, affordable, able to run without any intervention of the fishermen neither trouble of their fishing activity). In the present study, we are focusing on sensors for physical environmental data. These sensors, fixed on fishing gears, are profiling temperature, depth, salinity and turbidity (on selected vessels). Data are collected at the bottom and along the water column. They are transmitted to a data station on board before sending measurements to main databases on land via the GPRS network when available. This data flux is then close to real time and it allows monitoring the hydrological structures. Figure 4.6.1 displays position of collected profiles in 2008 (Figure 4.6.1a) and 2010 (Figure 4.6.1b). During these years, the number of valid profiles was increasing with 1145 profiles in 2008, 2551 profiles in 2009 and 3179 profiles in 2010. Following fishing areas, profiles are mainly located South of Brittany, in the Celtic Sea and in the western part of the Channel in 2008 (Figure 4.6.1a). In 2010, an increase in the number of collected profiles is observed with an

extent of areas covered by equipped fishing vessels. Indeed, data along the South-West French coast have been collected as well as new data further offshore in Celtic Sea and in the Eastern part of the Channel (Figure 4.6.1b). The spatial and temporal distribution of RECOPESCA profiles allows exploring the main features of the vertical hydrological structures (LeBlond et al., 2010).

4.7. North Sea (HZG)

4.7.1 Model description

Numerical simulations were performed using the 3D primitive equation General Estuarine Transport Model (GETM, Burchard and Bolding, 2002). The nested-grid model consists of a coarse-resolution North Sea-Baltic Sea (3 nautical miles) outer model, and a nested German Bight model with a horizontal resolution of about 1 km (Figure 4.7.1). Both models have 21 layers in generalized coordinates. The horizontal discretization is done on a spherical grid. The bathymetric data for both models are prepared using the ETOPO-1 topography, together with observations made available from the German Hydrographic Service (Bundesamt fuer Seeschifffahrt und Hydrographie, BSH; Dick et al., 2001).

The model system is forced by:

(1) The meteorological forcing derived from bulk formulae using wind, mean sea level pressure, air temperature, humidity and cloud cover taken from 1-hourly forecasts from the German Weather Service (DWD- COSMO-EU) with 7 km horizontal resolution,

(2) River inflow using climatological data for the 30 most important rivers within the North Sea-Baltic Sea model area provided by the Swedish Meteorological and Hydographical Institute (SMHI) and the BSH river-runoff data for the German Bight model setup

(3) Time varying lateral boundary conditions of sea surface elevations and salinity. The sea surface elevation, temperature and salinity of the western and northern open boundaries of the German Bight set-up is taken from the North Sea-Baltic Sea model output. The tidal forcing at the open boundaries of the North Sea-Baltic Sea model towards the Norwegian Sea and the English Channel was constructed from 13 partial tides from the TOPEX-POSEIDON data set.

The setup has been described in more detail by Staneva et al. (2009).

4.7.2 Data assimilation scheme

The German Bight circulation is rather complicated and there is a number of known error sources in the numerical models like e.g.,

- Uncertainties in the bathymetry
- Errors in the driving wind fields

- Errors in the bottom roughness parameterisation
- Uncertainties in the applied turbulence models
- Uncertainties in fresh water intake from rivers

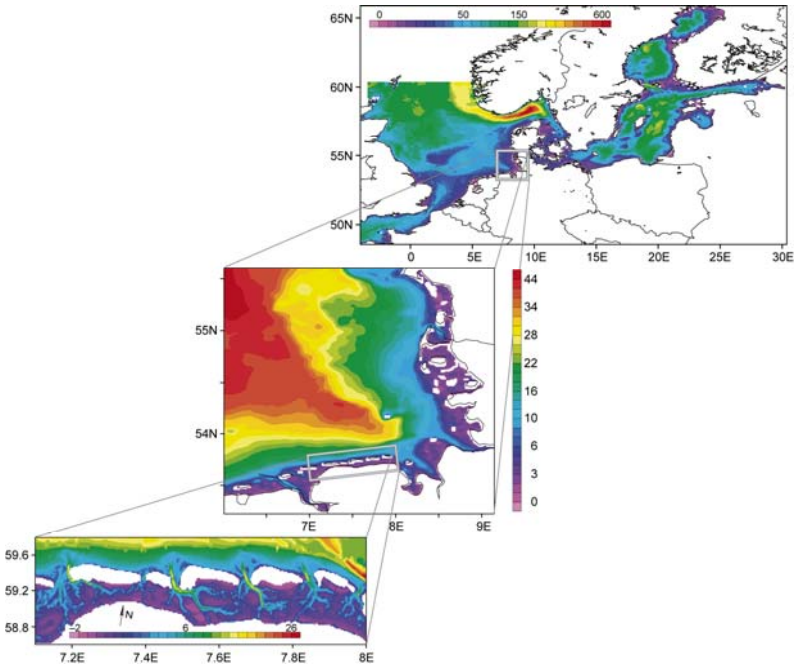

Figure 4.7.1: Nested Modelling System. Topography of the North Sea-Baltic Sea model (top); the German Bight (centre) and the Wadden Sea (bottom).

The German Bight has some characteristics features, which make the application of assimilation techniques to correct such errors quite demanding. For example due to the shallow water and the dominance of tides the memory of the system is relatively short. A study on the propagation of information provided by observations in time and space was conducted in Schulz-Stellenfleth and Stanev (2010).

One important component of the pre-operational COSYNA system is the generation of analysed surface current fields using numerical model data and HF radar measurements as input. The applied analysis technique is a spatio temporal optimal interpolation method, which has similarities to the method described in Barth et al. (2011). The basic idea is to process observation data and free model run data over an entire period in a single analysis step (Schulz-Stellenfleth, 2010). This approach proved to be very efficient in correcting phase and amplitude errors of the M2 tidal signal which is dominating the dynamics in the German Bight. In

the present setup 18 hrs hindcasts and 6 hrs forecasts are generated with hourly updates (see Figure 4.7.2 b). The data can be visualised and accessed on the COSYNA data portal (www.cosyna.de).

It was shown that the technique is able to improve the agreement with both the radar data and independent ADCP measurements, which were not used in the analysis. There are ongoing activities concerning validation using glider and shipborne ADCP data.

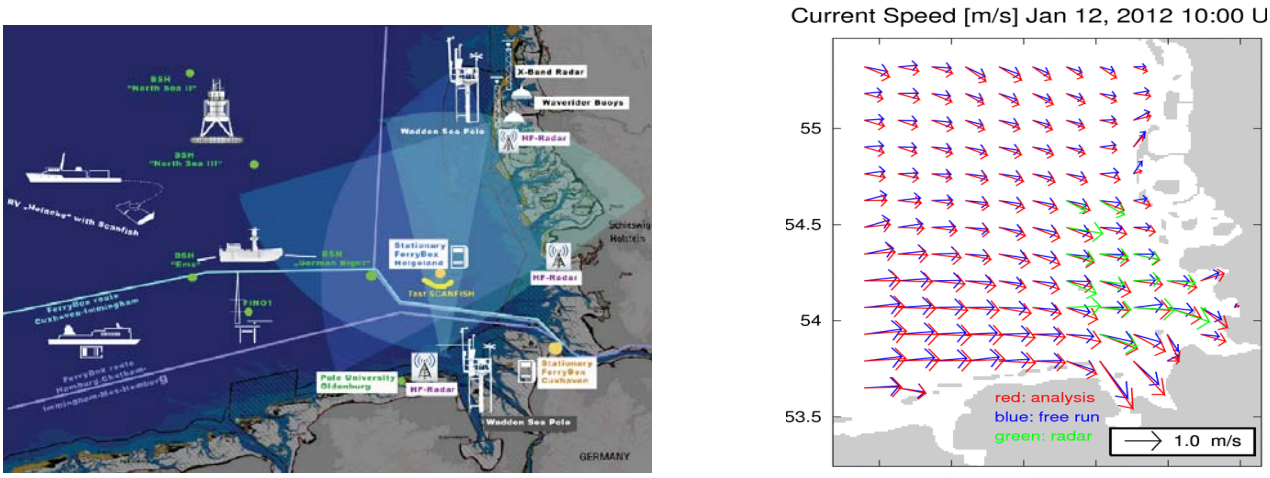

Figure 4.7.2: (left) COSYNA observing system, (right) Example of surface current analysis using GETM data and HF radar measurements as input.

The assimilation system is currently extended using additional temperature and salinity measurements from FerryBox systems (Grayek et al. 2011). In parallel analysis techniques are developed for glider data, which have recently become available.

4.7.3 Observational data sets

COSYNA is operated by the Institute for Coastal Research, Geesthacht in cooperation with the German Marine Research Consortium. It consists of observational nodes, data management systems and data assimilation capabilities, meeting thus the needs for high quality operational products in the German Bight. Synoptic now-casts and short-term forecasts of surface currents with high spatial and temporal resolution present the first products developed in the frame of COSYNA. Some methodological details associated with data assimilation were presented in Stanev et al. (2011).

COSYNA operates spatially distributed platforms with a multitude of sensors. Individual in-situ observing subsystems are: FerryBox operating on fixed routes, gliders, wave rider buoys and fixed sensor platforms. Remote sensing includes HF and X-band radar stations and data from satellites. Recently underwater node systems as sensor carrier as well as additionally lander systems have been added.

In the framework of the COSYNA project HF radar stations were installed at the islands of Wangerooge and

Sylt as well at the mainland near Buesum (see Figure 4.7.2 (left)). The Wangerooge station uses either 12.1 or 13.5 MHz depending on transmission and reception conditions. The corresponding radar wavelength range from 22 m to 28 m and the associated ocean wavelength relevant for the radar scattering process thus have wavelength between 11 m and 14 m. The depth of the ocean surface layer sensed by the radar can be estimated as approximately 1 m. Measurements are available every 20 min on a measurement grid with 2 km resolution.

5. Conclusions

In the report we describe all data assimilation systems that in WP9 perform OSE and OSSE experiments. They cover a large fraction of European coastal areas, starting from the Mediterranean Sea (the Adriatic and the Aegean Seas), North Atlantic Area (the Bay of Biscay and the North Sea) and the Baltic Sea. A common feature of all data assimilation systems is that they are based on models that simulate only physical processes. Therefore, the ongoing OSE and OSSE experiments estimate only the impact of existing and future coastal observational platforms that observe physical parameters. The major difference between the data assimilation systems is in the choice of the data assimilation schemes. Five systems apply Kalman Filter type data assimilation schemes. In particular data assimilation systems by the IFREMER, the MUM and the DELTARES are based on the Ensemble Kalman filter approach, the HCMR uses a space reduction approach for the estimation of background error covariances in the Kalman Filter, and the HGZ makes a temporally evolving estimate of background error covariances in order to simultaneously estimate several model states in a single step of the Kalman Filter. The remaining two data assimilation systems, applied by the DMI and the CMCC, use the three-dimensional variational approach. Following the different geographical and technical configuration of data assimilation systems OSE and OSSE experiments apply different approaches for the estimation of the observational impacts. They can, however, be divided into the two major groups: methods that are based on the estimate of the change of the error covariances of the analyses and the methods based on the direct comparison between observational and model estimates.

In the future presentation of the results of OSE and OSSE experiments we will have to underline the large variability of geographical areas and methodologies used for the estimation of the impact of observational systems. In addition we will have to cover as much as possible different environmental problems that our systems should address, from short term forecast in emergency situations to long term monitoring programmes.

References

Adcroft, A., Hill, C., Marshall, J., 1997, Representation of topography by shaved cells in a height coordinate ocean model. Mon. Weather Rev., 125, 2293-2315.

Barth, A., A. Alvera-Azca´rate, and R. H. Weisberg, 2008: Assimilation of high-frequency radar currents in a nested model of the West Florida Shelf, J. Geophys. Res., 113.

Barth, A. and Alvera-Azcarate, A. and Beckers, J. M. and Staneva, J. and Stanev, E. V. and Schulz-Stellenfleth, J., 2011: Correcting surface winds by assimilating high-frequency radar surface currents in the German Bight, Ocean Dynamics, 61, doi:10.1007/s10236-010-0369-0, 599-610.

Bennett, A. F., 1985: Array Design by Inverse Methods, Progress in Oceanography,15, 129-151.

Bennett AF (1990) Inverse methods for assessing ship-of-opportunity networks and estimating circulation and winds from tropical expendable bathythermograph data. J Geophys Res., 95:16111–16148.

Berg, P., Poulsen, J. W., 2011: Implementation details for HBM. DMI Technical Report No. 12-11, ISSN: 1399-1388, Copenhagen.

Besiktepe S., Ozsoy E., Unluata U., 1993: Filling the Marmara Sea by the Dardanelles lower layer inflow. Deep Sea Research I, Vol. 40, No.9, pp. 1815-1838

Breivik, O., and O. Satra (2001), Real time assimilation of HF radar currents into a coastal ocean model, J. Mar. Syst., 3– 4, 161–182.

Burchard, H. and Bolding, K., 2002 : GETM - a General Estuarine Transport Model, European Comission, No EUR 20253 EN, printed in Italy.

Byrd, R.H., Lu, P., Nocedal, J., Zhu, C.: A limited memory algorithm for bound constrained optimization. SIAM Journal on Scientific Computing 16, 1190-1208, 1995

Charria G., P. Lazure, B. Le Cann, A. Serpette, G. Reverdin, S. Louazel, F. Batifoulier, F. Dumas, A. Pichon, and Y. Morel (2011). Surface layer circulation derived from Lagrangian drifters in the Bay of Biscay. Journal of Marine Systems, in press.

Christensen O.B., M. Drews, J. H. ChristensenK. Dethloff, K. Ketelsen, I. Hebestadt, and A. Rinke, The HIRHAM Regional Climate Model Version 5 (β), DMI Tech. Rep. 06-17, pp22, 2006

Courtier, P., Th´epaut, J.-N. and Hollingsworth, A.: A strategy for operational implementation of 4D-Var, using an incremental approach. Q. J. R. Meteorol. Soc., 120, 1367–1388, 1994

Dick, S.K., Kleine, E., Mueller-Navarra, K., Klein, S. H., and Komo, H., 2001: The operational circulation model of BSH (BSHcmod) model description and validation, Bundesamt fuer Seeschifffahrt und Hydrographie (BSH),Hamburg, Report 29.

Drakopoulos, P.G., S.E.Poulos and A.Lascaratos, 1998: Buoyancy fluxes in the Aegean Sea. Rapp. Comm. Int. Mer. Medit., 35, 134-135.

Dobricic S., and N. Pinardi, 2008: An oceanographic three-dimensional assimilation scheme, Ocean Modelling, 22, 89-105.

Dobricic, S., Pinardi, N., Adani, M., Bonazzi, A., Fratianni, C., and M. Tonani, 2005: Mediterranean Forecasting System: An improved assimilation scheme for sea-level anomaly and its validation. Q. J. R. Meteor. Soc., 131, 3627-3642.

Dobricic, S., 2005, New mean dynamic topography of the Mediterranean calculated from assimilation system diagnostics, Geoph. Res. Lett., 32, L11606, doi:10.1029/2005GL022518.

Evensen, G.: Sequential data assimilation with a nonlinear quasi-geostrophic model using Monte Carlo methods to forecast error statistics, Journal of Geophysical Research, 99, 10 143- 10 162, 1994.

Grayek, S. and Staneva, J. and Schulz-Stellenfleth, J. and Petersen, W. and Stanev, E.V., 2011: Use of FerryBox surface temperature and salinity measurements to improve model based state estimates for the German Bight}, J. Marine Syst., doi:10.1016/j.jmarsys.2011.02.020, 88, 45-59.

Hoteit I., Pham, D.T. and J. Blum, 2002. A simplified reduced Kalman filtering and application to altimetric data assimilation in the Tropical Pacific. J. Mar. Sys. 36, 101-127.

Hoteit, I., Pham, D.T., Blum, J., 2003. A semi-evolutive filter with partially local correction basis for data assimilation in oceanography. Oceanol. Acta. 26, 511–524.

Lazure P., and F. Dumas (2008). An external-internal mode coupling for a 3D hydrodynamical model for applications at regional scale (MARS). Advances In Water Resources, 31(2), 233-250.

Leblond E., P. Lazure, M. Laurans, C. Rioual, P. Woerther, L. Quemener, and P. Berthou (2010). The Recopesca Project : a new example of participative approach to collect fisheries and in situ environmental data. CORIOLIS Quarterly Newsletter, (37), 40-48.

Le Hénaff, M., P. De Mey, and P. Marsaleix (2009). Assessment of observational networks with the Representer Matrix Spectra method—application to a 3D coastal model of the Bay of Biscay. Ocean Dynamics, 59(1), 3-20.

Kanarska, Y. and Maderich, V., 2008. Modelling of seasonal exchange flows through the Dardanelles Strait. Estuar. Coast. Shelf S., 79: 449-458.

Korres, G., A. Papadopoulos, P. Katsafados, D. Ballas, L. Perivoliotis and K. Nittis, 2011 .A 2-year intercomparison of the WAM-Cycle4 and the WAVEWATCH-III wave models implemented within the Mediterranean Sea. Mediterranean Marine Science, 12(1), 129-152.

Korres, G., K. Nittis, I. Hoteit and G.Triantafyllou, 2009. A high resolution data assimilation system for the Aegean Sea hydrodynamics. J. Mar. Sys. 77, 325-340.

Korres, G., and A.Lascaratos, 2003. A one-way nested eddy resolving model of the Aegean and Levantine basins: Implementation and climatological runs. Analles Geophysicae, MFSPP – Part I Special Issue, 21, 205-220.

Korres, G., A.Lascaratos, E. Hatziapostolou and P.Katsafados, 2002. Towards an Ocean Forecasting System for the Aegean Sea. The Global Atmosphere and Ocean System, Vol. 8, No. 2-3, 191-218.

Lekien, F. and Coulliette, C. and Bank, R. and Marsden, J. E. (2004) Open-boundary modal analysis: Interpolation, extrapolation, and filtering. Journal of Geophysical Research C, 109 (C12).

Lewis, J. K., I. Shulman, and A. F. Blumberg (1998), Assimilation of CODAR observations into ocean models, Cont. Shelf Res., 18, 541– 559.

Lipphardt, B. L., Jr., A. D. Kirwan Jr., C. E. Grosch, J. K. Lewis, and J. D. Paduan (2000), Blending HF radar and model velocities in Monterey Bay through normal mode analysis, J. Geophys. Res., 105(C2), 3425–3450,

Lorenc, A.C.: Development of an operational variational assimilation scheme. Journal of the Meteorological Society of Japan 75, 339-346, 1997

Luyten, P.: COHERENS – A coupled Hydrodynamical-Ecological Model for Regional and Shelf Seas: User Documentation. Version 2.1.2, RBINS-MUMM Report, Royal Belgian Institute of Natural Sciences, 2011

Madec G. 2008, ”NEMO ocean engine”. Note du Pole de modlisation, Institut Pierre-Simon Laplace (IPSL), France, No 27 ISSN No 1288-1619.

Mellor et al, 2002, Mellor, G. L., S. Hakkinen, T. Ezer and R. Patchen, 2002, A generalization of a sigma coordinate ocean model and an inter-comparison of model vertical grids, In: Ocean Forecasting: Conceptual Basis and Applications, N. Pinardi and J. D. Woods (Eds.), Springer, Berlin, 55-72, 2002.

Papadopoulos, A., G. Kallos, P. Katsafados, S. Nickovic, 2002. The Poseidon weather forecasting system: an overview. Glob. Atmos. Ocean Sys., 8, 218-237.

Pasaric, M., 2004. Annual cycle of river discharge along the Adriatic coast of Croatia. In: 37th Congress, Proceedings, vol. 37, CIESM.

Pinardi, N., Allen, I., Demirov, E., De Mey, P., Korres, G., Lascaratos, A., Le Traon, P.-Y., Maillard, C., Manzella, G., and Tziavos, C., 2003. The Mediterranean ocean forecasting system: first phase of implementation (1998–2001), Ann. Geophys., 21, 3–20.

Pham, D., J. Verron, and M.-C. Roubaud, 1997. A singular evolutive extended Kalman filter for data assimilation in oceanography. J. Mar. Sys., 16 (3-4), 323-340.

Port, A. and Gurgel,K.W. and Staneva, J. and Schulz-Stellenfleth, J. and Stanev,E.V., 2011: Tidal and wind-driven surface currents in the German Bight: HFR observations versus model simulations, Ocean Dynamics, doi:10.1007/s10236-011-0412-9, pp 1-19.

Poulos, S.E., P.G.Drakopoulos and M.B.Collins, 1997: Seasonal variability in the sea surface oceanographic conditions in the Aegean Sea (Eastern Mediterranean). An Overview. J. Mar. Systems, 13, 225-244.

Schulz-Stellenfleth, J. and Stanev, E.V., 2010: Statistical assessment of ocean observing networks - A study of water level measurements in the German Bight, Ocean Modelling, 10.1016/j.ocemod.2010.03.001}, 33, pp 270-282.

Schulz-Stellenfleth, J. and Wahle, K. and Staneva, J. and Seemann, J. and Cyseswki, M. and Gurgel, K.W. and Schlick, T. and Ziemer, F. and Stanev, E.V., 2010: Nutzung eines HF-Radarsystems zur Beobachtung und Vorhersage Stroemungen in der Deutschen Bucht im Rahmen von COSYNA, Deutsche Gesellschaft fuer Meereskunde, 3/10, pp 3-8,

Stanev, E.V. and Schulz-Stellenfleth, J. and Staneva, J. and Grayek, S. and Seemann, J. and Petersen, W., 2011: Coastal Observing and Forecasting System for the German Bight. Estimates of Hydrophysical States, Ocean Science, 7, pp 1-5, doi:10.5194/os-7-1-2011.

Staneva, J. and Stanev, E. and Wolff, J.-O. and Badewien, T. H. and Reuter, R. and Flemming, B. and Bartholomae, A. and Bolding, K., 2009 : Hydrodynamics and sediment dynamics in the German Bight. A focus on observations and numerical modeling in the East Frisian Wadden Sea, Cont. Shelf Res., 29, pp 302-319.

Sumihar, J.H. and M. Verlaan, 2010: Observation sensitivity analysis, Developing tools to evaluate and improve monitoring networks, Deltares report no. 1200087-000, 35 pages.

Verlaan, M., A. Zijderveld, H. de Vries, and J. Kroos, 2005, Operational storm surge forecasting in the Netherlands: developments in the last decade. Phil. Trans. R. Soc. A, 363, No. 1831, 1441-1453.

Verlaan, M., N. van Velzen, S. Hummel, and H. Gerritsen, 2010, OpenDA, a generic toolbox for data assimilation in numerical modelling. Presented at JonsMod workshop May 2010.

Zhuang,S.Y., Fu,W.W., and She, J.: A pre-operational 3-D variational data assimilation system in the North/Baltic Sea, Ocean Sci. Discuss., 8, 1131-1160, doi:10.5194/osd-8-1131-2011, 2011.

Zijl, F., R. Plieger, D. Vatvani, M. Verlaan, H. Gerritsen, and D. Twigt, 2008, DCSM v6 model setup and calibration of tidal propagation, Technical Report, Deltares 2008.